

Fluctuations of Random Matrix Products and 1D Dirac Equation with Random Mass

Kabir Ramola · Christophe Texier

Received: 11 May 2014 / Accepted: 24 July 2014 / Published online: 20 August 2014
© Springer Science+Business Media New York 2014

Abstract We study the fluctuations of certain random matrix products $\Pi_N = M_N \cdots M_2 M_1$ of $SL(2, \mathbb{R})$, describing localisation properties of the one-dimensional Dirac equation with random mass. In the continuum limit, i.e. when matrices M_n 's are close to the identity matrix, we obtain convenient integral representations for the variance $\Gamma_2 = \lim_{N \rightarrow \infty} \text{Var}(\ln \|\Pi_N\|)/N$. The case studied exhibits a saturation of the variance at low energy ε along with a vanishing Lyapunov exponent $\Gamma_1 = \lim_{N \rightarrow \infty} \ln \|\Pi_N\|/N$, leading to the behaviour $\Gamma_2/\Gamma_1 \sim \ln(1/|\varepsilon|) \rightarrow \infty$ as $\varepsilon \rightarrow 0$. Our continuum description sheds new light on the Kappus–Wegner (band center) anomaly.

Keywords Random matrix products · Lyapunov exponent · Generalised Lyapunov exponent · Dirac equation · Quantum localisation · Stochastic processes

1 Introduction

Transfer matrices lead to a convenient formulation of many statistical physics problems and have been extensively used since their introduction in the context of the Ising model [1]. In the presence of randomness, most of the physics is captured by the Lyapunov exponent Γ_1 which quantifies the growth rate of the matrix elements of a random matrix product (RMP) $\Pi_N = M_N \cdots M_2 M_1$. Given the measure characterizing the independent and identically distributed random matrices M_n 's, the Furstenberg formula allows one to obtain, at least in principle, the Lyapunov exponent $\Gamma_1 = \lim_{N \rightarrow \infty} \ln \|\Pi_N\|/N$, where $\|\cdot\|$ is a suitable norm, in terms of the solution of the Furstenberg's integral equation [2]. Besides the Lyapunov exponent,

K. Ramola · C. Texier (✉)
Laboratoire de Physique Théorique et Modèles Statistiques,
Univ. Paris Sud, CNRS, UMR 8626, 91405 Orsay cedex, France
e-mail: christophe.texier@u-psud.fr

K. Ramola
e-mail: kabir.ramola@u-psud.fr

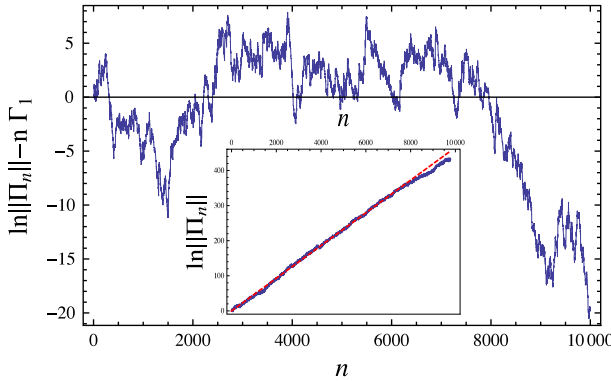


Fig. 1 (Color online) Fluctuations of a particular sequence of matrix products $\Pi_n = M_n \cdots M_1$, with matrices of the form (1.1)

which describes the *mean* free energy of the random Ising model [3–5], the *fluctuations* of RMP (Fig. 1) also play an important role and are the main subject of this paper.

The study of fluctuations is related to the generalised Lyapunov exponent analysis [3,4]¹ and the multifractal formalism introduced by Paladin and Vulpiani [6,7]. Fluctuations are of particular importance in the context of quantum localisation, where they dominate several physical quantities, like the local density of states [8] or the Wigner time delay [9]. Their precise characterisation is an important issue at the heart of the scaling approach used in the justification of the single parameter scaling (SPS) hypothesis (cf. Refs. [10,11] and references therein). In the last decade, this question has been re-examined more precisely for a lattice model [12–14]. Recently Lyapunov exponents have been analytically obtained for general RMPs of $SL(2, \mathbb{R})$ in the *continuum limit* [15]. This has significantly improved our understanding of RMPs and of one-dimensional (1D) quantum localisation models due to their close connection [16]. The present work is a first step towards generalising this approach for the fluctuations. We will consider matrices belonging to two particular subgroups of $SL(2, \mathbb{R})$:

$$M_n = \begin{pmatrix} \cos \theta_n & -\sin \theta_n \\ \sin \theta_n & \cos \theta_n \end{pmatrix} \begin{pmatrix} e^{\eta_n} & 0 \\ 0 & e^{-\eta_n} \end{pmatrix} \tag{1.1}$$

or

$$M_n = \begin{pmatrix} \cosh \tilde{\theta}_n & \sinh \tilde{\theta}_n \\ \sinh \tilde{\theta}_n & \cosh \tilde{\theta}_n \end{pmatrix} \begin{pmatrix} e^{\eta_n} & 0 \\ 0 & e^{-\eta_n} \end{pmatrix}. \tag{1.2}$$

We will show in Sect. 2 that products of matrices of the type (1.1) are transfer matrices for the bi-spinor $\Psi = (\psi, \chi)$ solution of the 1D Dirac equation

$$[\sigma_2 i\partial_x + \sigma_1 m(x)] \Psi(x) = \varepsilon \Psi(x) \tag{1.3}$$

for a mass of the form $m(x) = \sum_n \eta_n \delta(x - x_n)$ and with $\theta_n = \varepsilon (x_{n+1} - x_n) \in \mathbb{R}$, where σ_i 's are Pauli matrices. Matrices of the type (1.2) with $\tilde{\theta}_n = -i\varepsilon (x_{n+1} - x_n)$ correspond to the case $\varepsilon \in i\mathbb{R}$. The Dirac equation (1.3) with random mass is a relevant model in several

¹ Generalised central limit theorems for matrices was discussed in the mathematical literature (chapter V of the monograph [2]).

contexts of condensed matter, e.g. random spin chains or organic conductors (see references in Refs. [17, 18]). It can also be exactly mapped onto supersymmetric quantum mechanics [19] and the Sinai problem of 1D classical diffusion in a random force field [17, 20]. Many properties of the model can be obtained exactly when the mass is chosen to be a Gaussian white noise:

$$\langle m(x) \rangle = \mu g \text{ and } \langle m(x)m(x') \rangle_c = g \delta(x - x'), \tag{1.4}$$

where $\langle XY \rangle_c = \langle XY \rangle - \langle X \rangle \langle Y \rangle$. For example the Lyapunov exponent, defined in the localisation problem as $\gamma_1 = \lim_{x \rightarrow \infty} \ln |\psi(x)|/x$, is known [20]

$$\gamma_1 = -\mu g + \varepsilon \frac{H_{\mu+1}^{(1)}(\varepsilon/g)}{H_{\mu}^{(1)}(\varepsilon/g)}, \tag{1.5}$$

where $H_{\mu}^{(1)}(z)$ is the Hankel function. The case $\langle m(x) \rangle = 0$ is of particular interest since the Lyapunov exponent vanishes as $\varepsilon \rightarrow 0$, indicating a *delocalisation* point in the spectrum. In this unusual case, the characterisation of $\gamma_2 = \lim_{x \rightarrow \infty} \text{Var}(\ln |\psi(x)|)/x$ (i.e. $\Gamma_2 = \lim_{N \rightarrow \infty} \text{Var}(\ln \|\Pi_N\|)/N$) is thus crucial. We will show that the fluctuations saturate as $\varepsilon \rightarrow 0$, and thus dominate localisation properties.

2 Mapping

The mapping between RMP and 1D localisation models like the random Kronig–Penney model [3], was recently extended to general RMPs of $SL(2, \mathbb{R})$ [16]. For the case of interest here, the mapping works as follows: consider a random mass given as a superposition of delta-functions $m(x) = \sum_n \eta_n \delta(x - x_n)$, where coordinates are ordered $x_1 < x_2 < \dots$. Matching conditions across each impurity read $\psi(x_n^+) = \psi(x_n^-)e^{\eta_n}$ and $\chi(x_n^+) = \chi(x_n^-)e^{-\eta_n}$, hence the diagonal matrix in (1.1), while the rotation of angle $\theta_n = \varepsilon(x_{n+1} - x_n)$ stands for the free evolution between two impurities. If we consider the Dirac equation with a purely imaginary energy $\varepsilon \in i\mathbb{R}$, the matrix (1.2) with $\hat{\theta}_n = -i\theta_n \in \mathbb{R}$, relates $(\psi, \tilde{\chi}) = (\psi, -i\chi)$ at x_n^- and x_{n+1}^- .² The product $\Pi_N = M_N \dots M_2 M_1$ thus controls the value of the spinor and the study of the growth of the RMP characterizes the localisation properties of the wave function. It is convenient to introduce the Riccati variable $z(x) = -\varepsilon \chi(x)/\psi(x)$; from Eq. (1.3), we find

$$\frac{d}{dx} z(x) = -\varepsilon^2 - z(x)^2 - 2z(x)m(x). \tag{2.1}$$

If the lengths $\ell_n = x_{n+1} - x_n > 0$ are either equal (lattice) or distributed with an exponential law $P(\ell) = \rho e^{-\rho\ell}$, the stochastic differential equation (SDE) defines a Markov process. Hence, $\Psi(x_{N+1}^-) = \Pi_N \Psi(x_1^-)$ shows that $\ln \|\Pi_N\|$ and $\ln |\psi(x)|$ are asymptotically equivalent, thus their cumulants are related by $\gamma_n = \rho \Gamma_n$. In the following we will consider the continuum limit of the RMP problem when the random parameters are small $\theta_n = \varepsilon \ell_n \rightarrow 0$ and $\eta_n \rightarrow 0$, i.e. the matrices M_n are close to the identity matrix, in such a way that $\langle \eta_n \rangle = 0$ and $g = \langle \eta_n^2 \rangle / \langle \ell_n \rangle$ is fixed; this limit corresponds to the case where $m(x)$ is a Gaussian white noise with zero mean [15, 21].

The SDE (2.1) must be interpreted in the Stratonovich convention as is usual in physical problems [22]. The study of the fluctuations of the RMP can be performed by introducing

² Note that matrices (1.2) with $\tanh \hat{\theta}_n = e^{-2\beta J_n}$ and $\eta_n = \beta h_n$ are transfer matrices for the random Ising chain with couplings J_n and magnetic fields h_n [3]; a continuum approximation of the model was considered in Ref. [5] allowing these authors to recover the Lyapunov exponent (1.5) obtained first in Ref. [20].

the generalised Lyapunov exponent [4, 7]

$$\Lambda(q) = \lim_{x \rightarrow \infty} \frac{\ln \langle |\psi(x)|^q \rangle}{x} = \sum_{n=1}^{\infty} \frac{q^n}{n!} \gamma_n, \tag{2.2}$$

which is the generating function for the cumulants of $\ln |\psi(x)|$. In the following discussion we focus on γ_2 . From the definition of the Riccati variable, we may write $\ln |\psi(x)| = \int_0^x dt [z(t) + m(t)]$, hence

$$\gamma_2 = g + 2 \lim_{x \rightarrow \infty} \int_0^x dt \langle z(x) [z(t) + m(t)] \rangle_c. \tag{2.3}$$

It is convenient to use the relation

$$2 \int_{x_0}^x dt [z(t) + m(t)] = - \ln \left| \frac{z(x)}{z(x_0)} \right| + \int_{x_0}^x dt \left(z(t) - \frac{\varepsilon^2}{z(t)} \right), \tag{2.4}$$

obtained by integration of (2.1). Finally we get

$$\gamma_2 = g - \langle z \ln |z/\varepsilon| \rangle + \int dz dz' z G(z|z') \left(z' - \frac{\varepsilon^2}{z'} \right) f(z'). \tag{2.5}$$

The propagator is defined as

$$G(z|z') = \int_0^{\infty} dx [P_x(z|z') - f(z)] \tag{2.6}$$

where $P_x(z|z')$ is the conditional probability, solution of the Fokker–Planck equation $\partial_x P_x(z|z') = \mathcal{G}^\dagger P_x(z|z')$, and $f(z) = \lim_{x \rightarrow \infty} P_x(z|z')$ is the stationary distribution of the Riccati variable, with

$$\mathcal{G}^\dagger = 2g \partial_z z \partial_z z + \partial_z (z^2 + \varepsilon^2) \tag{2.7}$$

being the forward generator of the diffusion (adjoint of the generator). Equation (2.5) is one of our main results: f can be explicitly obtained as the normalisable solution of $\mathcal{G}^\dagger f = 0$ and G solves

$$\mathcal{G}^\dagger G(z|z') = f(z) - \delta(z - z'). \tag{2.8}$$

Note that, in the derivation of the second term of (2.5), we have used the underlying supersymmetry of the Dirac equation [16, 21] $f(z) = f(-\varepsilon^2/z) |\varepsilon|^2/z^2$, leading to $\langle \ln |z| \rangle = \ln |\varepsilon|$. Solving the equation for G , we can obtain an explicit representation for γ_2 in terms of multiple integrals, like it is done for another subgroup of $SL(2, \mathbb{R})$ in Appendix 3. We prefer to proceed in a different manner in order to derive limiting values for γ_2 .

3 Universal Regime (Large Real Energy $\varepsilon \gg g$)

The large energy limit is the *universal* regime where SPS holds [11]: a unique scale controls the average and the fluctuations $\gamma_2 \simeq \gamma_1$. The variance was explicitly calculated for this model in Ref. [23] and coincides with the known value for the Lyapunov exponent [20], Eq. (1.5), that saturates at high energy: $\gamma_2 \simeq g/2$ (Fig. 2).

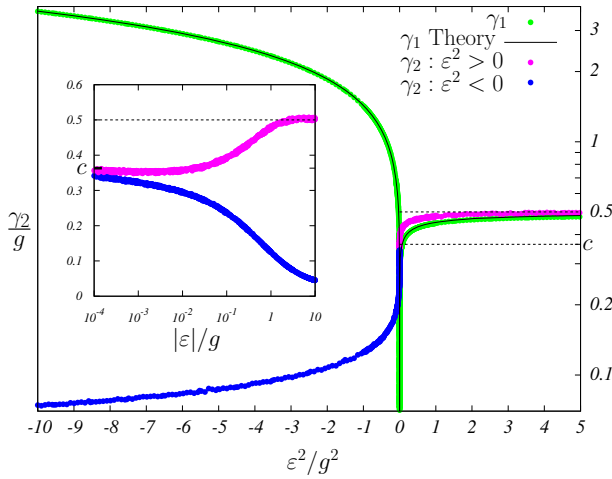


Fig. 2 (Color online) Plot of the Lyapunov exponent (γ_1) and the variance (γ_2). The *solid black line* corresponds to the exact result (1.5). For $|\varepsilon| \rightarrow 0$, γ_1 vanishes while the variance saturates to $c = 1 - 2/\pi$. *Inset* Plot in log-linear scale showing the low energy saturation of γ_2

4 Small Real Energy $\varepsilon \ll g$

The process $z(x)$ flows through the full interval \mathbb{R} and it is convenient to consider the variable

$$\zeta = \mp \ln(\pm z/|\varepsilon|)/2 \text{ for } z \in \mathbb{R}_{\pm} \tag{4.1}$$

When $z(x)$ goes from $+\infty$ to 0 the process $\zeta(x)$ crosses \mathbb{R} once, and a second time when $z(x)$ goes from 0 to $-\infty$. The new process obeys the SDE

$$\frac{d}{dx} \zeta(x) = -U'(\zeta(x)) + m(x) \tag{4.2}$$

for the unbounded potential

$$U(\zeta) = -\frac{|\varepsilon|}{2} \sinh 2\zeta. \tag{4.3}$$

Rewriting (2.5) in terms of the new variable, we get

$$\gamma_2 = g - 2 \langle \zeta U'(\zeta) \rangle + 8 \int d\zeta d\zeta' U(\zeta) \mathcal{G}(\zeta|\zeta') U(\zeta') \mathcal{P}(\zeta') \tag{4.4}$$

where $\mathcal{G}^\dagger \mathcal{P} = 0$ and

$$\mathcal{G}^\dagger \mathcal{G}(\zeta|\zeta') = \mathcal{P}(\zeta) - \delta(\zeta - \zeta') \tag{4.5}$$

for the forward generator

$$\mathcal{G}^\dagger = \frac{g}{2} \partial_\zeta^2 + \partial_\zeta U'(\zeta). \tag{4.6}$$

The details of the derivation of Eq. (4.4) are given in Appendix 1. The variable ζ is appropriate for the low energy analysis: the exponential dependence of the potential clearly illustrates the decoupling between the “deterministic force” $U'(\zeta)$ and Langevin “force” $m(x)$. We can map the problem onto an effective free diffusion problem in the interval $[\zeta_-, \zeta_+]$, where $\zeta_{\pm} =$

$\pm \ln(2g/|\varepsilon|)/2$. The form of $\mathcal{U}(\zeta)$ at infinity leads to the boundary conditions: absorption at one boundary, $\mathcal{P}(\zeta_+) = 0$, with reinjection of the current at the other boundary, $\mathcal{P}'(\zeta_-) = \mathcal{P}'(\zeta_+)$. The stationary distribution takes the approximate form

$$\mathcal{P}(\zeta) \simeq \frac{2(\zeta_+ - \zeta)}{(\zeta_+ - \zeta_-)^2} \text{ for } \zeta \in [\zeta_-, \zeta_+] \tag{4.7}$$

and the solution of Eq. (4.5) is given by

$$\mathcal{G}(\zeta|\zeta') \simeq \frac{2}{g} \left\{ -\frac{1}{6}(\zeta_+ - \zeta) + \frac{1}{3(\zeta_+ - \zeta_-)^2} \left[(\zeta_+ - \zeta_>)^3 + 3(\zeta_< - \zeta_-)^2(\zeta_+ - \zeta_>) + \theta_H(\zeta' - \zeta) (\zeta' - \zeta)^3 \right] \right\}, \tag{4.8}$$

where $\theta_H(\zeta)$ is the Heaviside function, $\zeta_> = \max(\zeta, \zeta')$ and $\zeta_< = \min(\zeta, \zeta')$. As a check, we recover that the Lyapunov exponent

$$\gamma_1 = 2 \langle \mathcal{U}(\zeta) \rangle \tag{4.9}$$

vanishes as

$$\gamma_1 \underset{|\varepsilon| \rightarrow 0}{\simeq} \frac{g}{\ln(2g/|\varepsilon|)}, \tag{4.10}$$

a behaviour which coincides with the asymptotic of the exact result (1.5). We easily compute (4.4), leading to

$$\gamma_2 \underset{\varepsilon \rightarrow 0}{\simeq} g \left[\frac{1}{3} + \frac{1}{2 \ln(2g/|\varepsilon|)} \right], \tag{4.11}$$

which shows the *saturation* of the fluctuations as $\varepsilon \rightarrow 0$.

5 Small Complex Energy $-i\varepsilon \ll g$

For complex energy $\varepsilon \in i\mathbb{R}$, the process $z(x)$ is trapped on \mathbb{R}_+ . The SDE (4.2) still holds for the bounded potential

$$\mathcal{U}(\zeta) = \frac{|\varepsilon|}{2} \cosh 2\zeta. \tag{5.1}$$

Making use of the fact that $\mathcal{U}(\zeta)$ is symmetric, we can show that the representations (4.4) and (4.9) are still valid (see Appendix 1), the stationary distribution being now an equilibrium distribution $\mathcal{P}(\zeta) \propto \exp[-2\mathcal{U}(\zeta)/g]$. In the low energy limit, we again use the decoupling between the deterministic force and the Langevin force: the effect of the confining potential is now replaced by reflecting boundary conditions $\mathcal{P}'(\zeta_-) = \mathcal{P}'(\zeta_+) = 0$. The stationary distribution is

$$\mathcal{P}(\zeta) \simeq \frac{1}{\zeta_+ - \zeta_-} \text{ for } \zeta \in [\zeta_-, \zeta_+], \tag{5.2}$$

thus (4.9) again leads to (4.10). The propagator takes the form

$$\mathcal{G}(\zeta|\zeta') \simeq \frac{2}{g} \left\{ -\frac{|\zeta - \zeta'|}{2} + \frac{\zeta^2 + \zeta'^2}{2(\zeta_+ - \zeta_-)} + \frac{\zeta_+ - \zeta_-}{12} \right\} \tag{5.3}$$

and Eq. (4.4) gives

$$\gamma_2 \underset{\varepsilon \rightarrow i0}{\simeq} g \left[\frac{1}{3} - \frac{1}{2 \ln(2g/|\varepsilon|)} \right]. \tag{5.4}$$

This shows that, as a function of ε^2 , the variance γ_2 is continuous around 0. Setting $\varepsilon = 0$, a more direct analysis can be performed (Appendix 2) showing that

$$\gamma_2 = g \left(1 - \frac{2}{\pi} \right) \simeq 0.363 g \text{ for } \varepsilon = 0. \tag{5.5}$$

The small discrepancy ($\sim 8\%$) is explained by the fact that the constant term in (4.11, 5.4) is sensitive to the precise position of the cutoffs ζ_{\pm} of the free diffusion approximation. Numerical calculations confirm the saturation and suggest a logarithmic behaviour, although it is difficult to precisely fit this logarithmic correction (Fig. 2).

6 Large Complex Energy $-i\varepsilon \gg g$: A Perturbative Treatment of the Stochastic Differential Equation

In this case, it is convenient to develop a perturbative approach based on the SDE (2.1). We perform the rescaling

$$z(x) = |\varepsilon| + \sqrt{g|\varepsilon|} y(u) \text{ with } x = u/|\varepsilon|, \tag{6.1}$$

leading to

$$\frac{dy(u)}{du} = -2y(u) - 2\eta(u) - \alpha [y(u)^2 + 2y(u)\eta(u)], \tag{6.2}$$

where $\eta(u)$ is a normalised Gaussian white noise, $\langle \eta(u)\eta(u') \rangle = \delta(u - u')$. The perturbative parameter is $\alpha = \sqrt{g/|\varepsilon|}$. Expansion of the process in powers of α , as $y = y_0 + y_1 + y_2 + \dots$, leads to the explicit integral representations

$$y_0(u) = -2 \int_0^u dt e^{-2(u-t)} \eta(t), \tag{6.3}$$

$$y_1(u) = -\alpha \int_0^u dt e^{-2(u-t)} [y_0(t)^2 + 2y_0(t)\eta(t)], \tag{6.4}$$

$$y_2(u) = -2\alpha \int_0^u dt e^{-2(u-t)} [y_0(t) + \eta(t)] y_1(t), \tag{6.5}$$

where transient terms have been neglected. Order zero $y_0(u)$ is the Ornstein–Uhlenbeck process. These expressions are suitable for computing $\gamma_1 = \langle z \rangle \simeq |\varepsilon| + \sqrt{g|\varepsilon|} \langle y_1(u) \rangle = |\varepsilon| + g/2$ and the correlator (2.3). The latter can be rewritten in terms of the rescaled process as

$$\gamma_2 = g \left\{ 1 + 2 \int_0^\infty du \langle y(u_0)y(u + u_0) \rangle_c + 2 \langle y(u_0) \int_0^{u_0} du \eta(u) \rangle_c \right\}, \tag{6.6}$$

where $u_0 \rightarrow \infty$. It is easy to see that the first non-zero contribution to this expression comes at order α^2 . We then have the following expression for γ_2 to lowest order in α

$$\begin{aligned} \gamma_2 = 2g \left\{ \int_0^\infty du \left[\langle y_0(u_0)y_2(u + u_0) \rangle_c + \langle y_2(u_0)y_0(u + u_0) \rangle_c \right. \right. \\ \left. \left. + \langle y_1(u_0)y_1(u + u_0) \rangle_c \right] + \langle y_2(u_0) \int_0^{u_0} du \eta(u) \rangle_c + \mathcal{O}(\alpha^4) \right\}. \end{aligned} \tag{6.7}$$

It is possible to compute this expression exactly. Since the process is derived from a Gaussian white noise source, we can use Wick’s theorem to reduce all the correlation functions to products over two-point correlation functions. However, the full calculation is rather cumbersome. Instead, we use the stochastic calculus functionalities of `Mathematica 9.0` to derive the values of the correlators. We have

$$\lim_{u_0 \rightarrow \infty} \int_0^\infty du \left[\langle y_0(u_0)y_2(u + u_0) \rangle_c + \langle y_2(u_0)y_0(u + u_0) \rangle_c \right] = \frac{3}{4}\alpha^2, \tag{6.8}$$

$$\lim_{u_0 \rightarrow \infty} \int_0^\infty du \langle y_1(u_0)y_1(u + u_0) \rangle_c = \frac{1}{8}\alpha^2, \tag{6.9}$$

$$\lim_{u_0 \rightarrow \infty} \langle y_2(u_0) \int_0^{u_0} du \eta(u) \rangle_c = -\frac{3}{4}\alpha^2. \tag{6.10}$$

Summing these three contributions, we arrive at

$$\gamma_2 \underset{\varepsilon \rightarrow i\infty}{\simeq} \frac{g^2}{4|\varepsilon|}. \tag{6.11}$$

7 Numerical Calculations

7.1 Method

We have performed a Monte Carlo simulation of the matrix problem, i.e. of the Dirac equation for the random mass

$$m(x) = \sum_n \eta_n \delta(x - x_n), \tag{7.1}$$

where the impurities are independently and uniformly dropped on the line with a mean density ρ . This corresponds to an exponential distribution $P(\ell) = \rho e^{-\rho\ell}$ for the distance $\ell_n = x_{n+1} - x_n > 0$ between consecutive impurities. The mass is uncorrelated in space, i.e. is a *non-Gaussian* white noise. The limit of the Gaussian white noise considered in the previous sections corresponds to $\rho \rightarrow \infty$ and $\eta_n \rightarrow 0$ with $\langle \eta_n \rangle = 0$ and $g = \rho \langle \eta_n^2 \rangle$ fixed. This is a continuum model that is easy to implement numerically.

7.1.1 Real Energy

We parametrize the spinor as $\Psi = e^\xi (\sin \Theta, -\cos \Theta)$ and study the evolution of the two variables. Between impurities n and $n + 1$ we have obviously $\Theta_{n+1}^- - \Theta_n^+ = \varepsilon \ell_n$ and $\xi_{n+1}^- - \xi_n^+ = 0$, where we have introduced the notation $\Theta_n^\pm = \Theta(x_n^\pm)$ and $\xi_n^\pm = \xi(x_n^\pm)$. Across the impurity [24]

$$\tan(\Theta_n^+) = \tan(\Theta_n^-) e^{2\eta_n} \tag{7.2}$$

$$\xi_n^+ - \xi_n^- = \frac{1}{2} \ln [e^{2\eta_n} \sin^2 \Theta_n^- + e^{-2\eta_n} \cos^2 \Theta_n^+]. \tag{7.3}$$

The norm of the RMP is identified with the norm of the spinor

$$\ln \|\Pi_N\|_{\Psi_0} = \xi(x_{N+1}^-) = \frac{1}{2} \ln [\Psi(x_{N+1}^-)^\dagger \Psi(x_{N+1}^-)]. \tag{7.4}$$

7.1.2 Complex Energy

For $\varepsilon \in i\mathbb{R}$, we write the spinor as $\Psi = e^{\xi}(\sin \Theta, -i \cos \Theta)$. Evolution of the two variables due to the rotation of complex angle is [23]

$$\tan(\Theta_{n+1}^- + \pi/4) = \tan(\Theta_n^+ + \pi/4) e^{2|\varepsilon|\ell_n} \tag{7.5}$$

$$\xi_{n+1}^- - \xi_n^+ = \frac{1}{2} \ln [\cos 2\Theta_n^+ / \cos 2\Theta_{n+1}^-]. \tag{7.6}$$

Evolution across an impurity are similar to the case of real energy.

7.2 The Saturation of γ_2 for $\varepsilon \rightarrow i\infty$ when $m(x)$ is a Non-Gaussian White Noise

For large but finite density ρ we show that the fluctuations saturate for large complex energy $|\varepsilon| \gg \rho$. Expansion of the previous equations in the limit $|\varepsilon|\ell_n \rightarrow \infty$ gives $\xi_{n+1}^- - \xi_n^+ = |\varepsilon|\ell_n + \ln \cosh \eta_n + \mathcal{O}(e^{-2|\varepsilon|\ell_{n-1}}) + \mathcal{O}(e^{-2|\varepsilon|\ell_n})$. We deduce the following representation for the process $\xi(x)$

$$\xi(x) = |\varepsilon|x + \sum_{n=1}^{\mathcal{N}(x)} \ln \cosh \eta_n + \mathcal{O}\left(\frac{\rho}{|\varepsilon|}\rho x\right) \tag{7.7}$$

where $\mathcal{N}(x)$ is the number of impurities on the interval $[0, x]$. $\mathcal{N}(x)$ is a Poisson process and $\xi(x)$ a compound Poisson process (see for instance the introduction of Ref. [25] and references therein). Using standard properties of compound Poisson processes, we obtain

$$\gamma_1 = \lim_{x \rightarrow \infty} \frac{\xi(x)}{x} \simeq |\varepsilon| + \rho \langle \ln \cosh \eta_n \rangle \tag{7.8}$$

$$\gamma_2 = \lim_{x \rightarrow \infty} \frac{\text{Var}(\xi(x))}{x} \simeq \rho \langle \ln^2 \cosh \eta_n \rangle \tag{7.9}$$

(note that the *cumulants* of $\xi(x)$ involves the *moments* of the jump amplitudes). Hence for $|\varepsilon| \gg \rho$ with $\eta_n \ll 1$ we obtain $\gamma_1 \simeq |\varepsilon| + \rho \langle \eta_n^2 \rangle / 2 = |\varepsilon| + g/2$ and $\gamma_2 \simeq \rho \langle \eta_n^4 \rangle / 4$.

7.3 Results

As a first check, we compare the Lyapunov exponent γ_1 obtained from the procedure explained above with the analytical expression (1.5): green dots and black continuous line on Fig. 2, respectively. The agreement is excellent.

For large real energy we see on the figure that γ_2 saturates at the same value as γ_1 (SPS). For small energy, $|\varepsilon| \rightarrow 0$, the inset of Fig. 2 shows the logarithmic behaviours.

The behaviour (6.11) is more difficult to observe as it is a property of the Dirac equation when the mass $m(x)$ is a *Gaussian* white noise. The numerical simulation is performed for a *non-Gaussian* white noise, Eq. (7.1), which leads to a saturation of the fluctuations, as explained in paragraph 7.2. For this reason, the power law decay (6.11) is only obtained in an intermediate range of energy $g \ll |\varepsilon| \ll \rho$ (Fig. 3), and we observe the saturation for $|\varepsilon| \gg \rho$. Choosing weights distributed according to a symmetric exponential law like in Ref. [21], the saturation value is $\gamma_2 \simeq \rho \langle \eta_n^4 \rangle / 4 = 3g^2 / (2\rho)$, in agreement with the numerics (black dotted lines in Fig. 3).

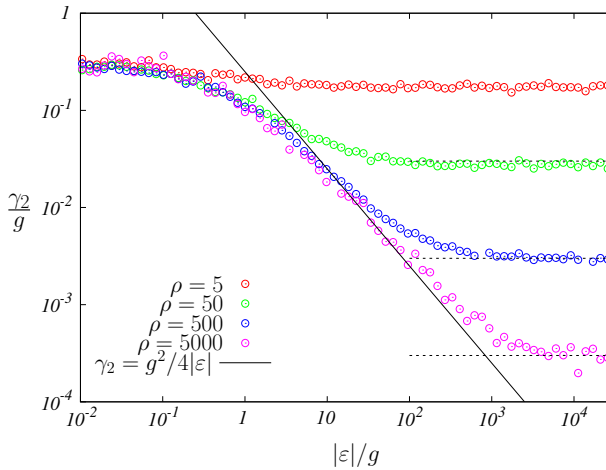


Fig. 3 (Color online) Variance for matrices of type (1.2) with exponentially distributed angles $\langle \bar{\theta}_n \rangle = |\varepsilon|/\rho$ and weights distributed according to a symmetric exponential law with $g = \rho \langle \eta_n^2 \rangle$. The saturation values are $\gamma_2 \simeq 3g^2/2\rho$ (dotted lines). The crossover between the two behaviours takes place at a scale $|\varepsilon| \sim \rho$

8 Localisation

8.1 Low Energy Localisation

The saturation of the fluctuations concomitant with the vanishing of the Lyapunov exponent has important consequences for the localisation. While the Lyapunov exponent is usually introduced as a measure of the localisation (see the monographs [3,26] or the review [21]), for a given small energy $|\varepsilon| \ll g$, the fluctuations dominate

$$\sqrt{\gamma_2 x} \gtrsim \gamma_1 x \text{ for } x \lesssim \xi_\varepsilon = (1/g) \ln^2(g/|\varepsilon|),$$

i.e. on a scale ξ_ε much larger than the inverse Lyapunov exponent $1/\gamma_1 \sim (1/g) \ln(g/|\varepsilon|)$. The scale ξ_ε has appeared in other studies: in the average Green’s function [20] (see discussion and references in Ref. [27]), in the distribution of the distances between consecutive nodes of the wave function [18], or in the boundary sensitive average local [28] and global density of states [18] (Thouless criterion). This is a new indication that *the Lyapunov exponent cannot be interpreted as the inverse localisation length in this case* [18,21].

8.2 Band Center Anomaly

The standard weak disorder expansion for the tight-binding (Anderson) model

$$-t \varphi_{n+1} + V_n \varphi_n - t \varphi_{n-1} = \varepsilon \varphi_n \tag{8.1}$$

is known to break down at the band center ($\varepsilon = 0$) [29,30]. Whereas the standard expansion gives [3,31] $\gamma_1 \simeq a \langle V_n^2 \rangle / (8t^2 \sin^2 \kappa)$ at $\varepsilon = -2t \cos \kappa$ for uncorrelated potentials V_n (a is the lattice spacing), the correct behaviour in the band center is $\gamma_1 = a [\Gamma(3/4)/\Gamma(1/4)]^2 \langle V_n^2 \rangle / t^2 + \mathcal{O}(\varepsilon)$ [31]. This small difference, 0.125 versus 0.114..., and

those of other physical quantities, have been referred to as band center “anomalies”³. This phenomenon may be easily analysed within our continuum description: the continuum limit of the Anderson model (8.1) near the band center ($\varepsilon \rightarrow 0$) is the random Dirac equation [32]

$$[-i\sigma_3 \partial_x + V_0(x) + \sigma_1 V_\pi(x)] \tilde{\Psi}(x) = \varepsilon \tilde{\Psi}(x) \tag{8.2}$$

(for $2at = 1$), where $V_0(x)$ and $V_\pi(x)$ describe forward and backward (umklapp) scattering, respectively. This makes it clear that the disorder cannot be treated perturbatively for $\varepsilon = 0$. After a rotation

$$\Psi = \frac{1}{\sqrt{2}}(1 - i\sigma_1) \tilde{\Psi} \tag{8.3}$$

and choosing $V_0(x) = \sum_n v_n \delta(x - x_n)$ and $V_\pi(x) = \sum_n \eta_n \delta(x - x_n)$, this disordered model can be described by transfer matrices (1.1), by setting the angles $\theta_n = \varepsilon(x_{n+1} - x_n) - v_n$. For $\varepsilon = 0$, the Lyapunov exponent in the continuum limit is expressed in terms of elliptic integrals (this case was considered in Sect. 6 of Ref. [15]):

$$\gamma_1 = g \left[\frac{1}{k^2} \left(\frac{\mathbf{E}(k)}{\mathbf{K}(k)} - 1 \right) + 1 \right] \text{ with } k = \frac{1}{\sqrt{1 + g_0/g}} \tag{8.4}$$

where $g = \rho \langle \eta_n^2 \rangle$ and $g_0 = \rho \langle v_n^2 \rangle$. For uncorrelated site potentials, $\langle V_n V_m \rangle \propto \delta_{n,m}$, we have $g_0 = g$; Eq. (8.4) with $k = 1/\sqrt{2}$ leads to $\gamma_1 = g [2\Gamma(3/4)/\Gamma(1/4)]^2$, in perfect correspondence with the result of Ref. [31]. γ_2 at the band center was found in Ref. [13] where it was shown that the anomaly is *small*, $\gamma_2/\gamma_1 \simeq 1.047$. On the other hand, the suppression of forward scattering⁴ ($g_0 \ll g$) leads to the model studied in the present paper with a *strong* anomaly $\gamma_2/\gamma_1 \sim \ln(g/g_0)$ at $\varepsilon = 0$ and $\gamma_2/\gamma_1 \sim \ln(g/|\varepsilon|)$ for $g_0 \ll |\varepsilon| \ll g$, Fig. 4 (the value of γ_2 for finite $g_0 \ll g$ is deduced from a continuity assumption). Our continuous description thus makes clear how one can tune the band center anomaly by adjusting the relative magnitude of forward and backward scattering.

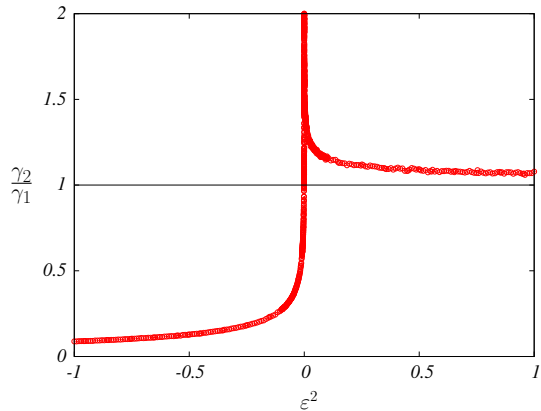
9 Conclusion

In this paper we have characterized the statistical properties of random matrix products $\Pi_N = M_N \cdots M_2 M_1$ for two subgroups of $SL(2, \mathbb{R})$, by making use of the fact that, for a certain choice of the distribution of the angles in (1.1) and (1.2), $\ln \|\Pi_N\|$ can be simply expressed in terms of a Markov process [15]. We have deduced the variance explicitly; the integral representations Eqs. (2.5, 4.4) were demonstrated to be convenient for extracting limiting behaviours. Following Ref. [7] and making use of (2.4), the generalised Lyapunov exponent (2.2) may be obtained as the largest eigenvalue of the operator $\mathcal{G}^\dagger + q(z - \varepsilon^2/z)/2$. The cumulants can be obtained by using the perturbative method used in Refs. [13,33], however, apart from γ_1 , this leads to integral representations that seem less convenient to handle. We have also obtained an integral representation similar to (2.5) in the case of two other particular subgroups of $SL(2, \mathbb{R})$ (see Appendix 3), corresponding to the model studied

³ As shown in Ref. [31], the occurrence of anomalies is not specific to the band center but is an effect of commensurability.

⁴ In the Anderson model, forward and backward scattering may be adjusted as follows: one considers random potentials $V_n = V_0(na) + (-1)^n V_\pi(na)$, where $V_0(x)$ and $V_\pi(x)$ are two independent random functions varying smoothly at the scale of the lattice spacing a . Forward scattering is controlled by the strength g_0 of $V_0(x)$ whereas backward scattering is due to anti-correlation of nearest neighbour potentials, described by $V_\pi(x)$ with strength g .

Fig. 4 (Color online) The ratio of the two first cumulants for the random mass Dirac model presents a logarithmic divergence for $|\varepsilon| \rightarrow 0$



in Ref. [33]. It remains a challenging issue to obtain a resolution of this problem, in the spirit of the general classification of Lyapunov exponents provided recently in Ref. [15].

Acknowledgments We acknowledge stimulating discussions with Alain Comtet, Bernard Derrida, Thierry Jolicœur and Satya Majumdar, and a helpful suggestion of Anupam Kundu.

Appendix 1: Details of the Derivation of Eq. (4.4)

$$\varepsilon^2 > 0$$

For real energy, we see from the SDE (2.1) that the process $z(x)$ flows towards \mathbb{R} . We have introduced the change of variable $\zeta = \mp \ln(\pm z/|\varepsilon|)/2$ for $z \in \mathbb{R}_\pm$, implying that the new process $\zeta(x)$ crosses \mathbb{R} twice when $z(x)$ does once. Hence the change of variable maps the SDE (2.1) onto the couple of SDEs

$$\frac{d}{dx}\zeta = |\varepsilon| \cosh 2\zeta \pm m(x) = -\mathcal{U}'_\pm(\zeta) + \sqrt{g} \eta(x). \tag{10.1}$$

In the main text we used $\langle m(x) \rangle = 0$ and the local nature of the mass correlation to disregard the sign. Here we consider for the moment the general case $\langle m(x) \rangle = \mu g$ and introduce a couple of potentials $\mathcal{U}_\pm(\zeta) = -(|\varepsilon|/2) \sinh 2\zeta \mp \mu \zeta$ related to the cases $z(x) > 0$ and $z(x) < 0$, respectively. $\eta(x)$ is a normalised Gaussian white noise with zero mean. The process is characterised by two stationary distributions $\mathcal{P}^\pm(\zeta)$, each normalized, related to $f(z)$ for $z \in \mathbb{R}_\pm$. For example, the Lyapunov exponent is given by [16]

$$\gamma_1 = \langle z + m(x) \rangle = \mu g + \frac{|\varepsilon|}{2} \left[\int d\zeta \mathcal{P}^+(\zeta) e^{-2\zeta} - \int d\zeta \mathcal{P}^-(\zeta) e^{+2\zeta} \right]. \tag{10.2}$$

Now considering the case $\mu = 0$ for which $\mathcal{P}^+ = \mathcal{P}^-$, leads to $\gamma_1 = -|\varepsilon| \langle \sinh 2\zeta \rangle$, i.e.

$$\gamma_1 = 2 \langle \mathcal{U}(\zeta) \rangle. \tag{10.3}$$

Fluctuations may be discussed in a similar way. A crucial observation is that, in the original SDE (2.1), the diffusion effectively vanishes at $z = 0$, implying the absence of correlations between the process at coordinates x and x' associated to $z(x) > 0$ and $z(x') < 0$. It follows

that the contributions of the fluctuations related to the two intervals $z \in \mathbb{R}_+$ and $z \in \mathbb{R}_-$ simply add. The second term of (2.5) takes the form

$$\frac{1}{2} \left(\int d\zeta d\zeta' |\varepsilon| e^{-2\zeta} \mathcal{G}^+(\zeta|\zeta') (-2|\varepsilon|) \sinh 2\zeta' \mathcal{P}^+(\zeta') + \int d\zeta d\zeta' (-|\varepsilon|) e^{+2\zeta} \mathcal{G}^-(\zeta|\zeta') (-2|\varepsilon|) \sinh 2\zeta' \mathcal{P}^-(\zeta') \right).$$

For $\mu = 0$ we have $\mathcal{G}^+ = \mathcal{G}^-$ leading to Eq. (4.4).

$$\varepsilon^2 < 0$$

For imaginary energy the analysis is slightly different: the process $z(x)$ is trapped on \mathbb{R}_+ and $\zeta(x)$ does not flow across \mathbb{R} . The change of variable is simply $\zeta = -(1/2) \ln(z/|\varepsilon|)$. The new process is trapped by the potential well $\mathcal{U}(\zeta) = (|\varepsilon|/2) \cosh 2\zeta - \mu\zeta$. The equilibrium distribution is $\mathcal{P}(\zeta) \propto \exp[-(2/g)\mathcal{U}(\zeta)]$. When $\mu = 0$ the potential is symmetric. We can symmetrize the expression $\gamma_1 = |\varepsilon| \langle e^{-2\zeta} \rangle$, leading to $\gamma_1 = |\varepsilon| \langle \cosh 2\zeta \rangle$, i.e. again to (10.3). Eq. (2.5) leads to

$$\gamma_2 = g + 2|\varepsilon| \langle \zeta e^{-2\zeta} \rangle + 2|\varepsilon|^2 \int d\zeta d\zeta' e^{-2\zeta} \mathcal{G}(\zeta|\zeta') \cosh 2\zeta' \mathcal{P}(\zeta'). \tag{10.4}$$

The second term can be obviously symmetrized, which gives the second term of (4.4). Symmetrization of the third integral term works as follows: the propagator may be decomposed over the left/right eigenvectors of the forward generator \mathcal{G}^\dagger as

$$\mathcal{G}(\zeta|\zeta') = \sum_{n>0} \frac{\Phi_n^R(\zeta)\Phi_n^L(\zeta')}{\mathcal{E}_n} \tag{10.5}$$

where $\mathcal{G}^\dagger \Phi_n^R(\zeta) = -\mathcal{E}_n \Phi_n^R(\zeta)$ and $\mathcal{G} \Phi_n^L(\zeta) = -\mathcal{E}_n \Phi_n^L(\zeta)$. Because the potential $\mathcal{U}(\zeta)$ is symmetric, the eigenvectors have a symmetry property $\Phi_n^{L/R}(-\zeta) = (-1)^n \Phi_n^{L/R}(\zeta)$. Integration over ζ' in (10.4) selects only the contributions of even eigenvectors which allows one to symmetrize the integrand with respect to $\zeta \rightarrow -\zeta$, leading to Eq. (4.4).

It is remarkable that despite the dynamics of the process $\zeta(x)$ being quite different for real and imaginary ε , we have found a unique representation for both γ_1 , Eq. (4.9), and γ_2 , Eq. (4.4), expressed in terms of the potential $\mathcal{U}(\zeta)$.

Appendix 2: Direct Calculation of γ_2 for $\varepsilon = 0$

The study of the case $\varepsilon = 0$ shows some subtlety related to the choice of the norm of the matrix. In the usual case, the statistical properties of the RMP are independent of the precise definition of the norm [2,4]. Bougerol and other authors propose

$$||M|| = \text{Sup}\{|Mx|, x \in \mathbb{R}^2, |x| = 1\} \tag{10.6}$$

where $|x|$ is the norm on the vector space.

In the numerical calculation, we have parametrized the spinor as $\Psi = e^{\xi} (\sin \Theta, -\cos \Theta)$, in the spirit of the phase formalism [26], and study the statistical properties of $\xi(x) = (1/2) \ln [\Psi(x)^\dagger \Psi(x)]$, usually setting $\Theta(0) = \Theta_0 = 0$. Let us discuss the general case where Θ_0 may differ from 0. Since $\Psi(x_{N+1}^-) = \Pi_N \Psi(x_1^-)$, the numerical procedure corresponds to considering the norm

$$||\Pi_N||_{\Psi_0} = |\Pi_N \Psi_0| \text{ with } \Psi_0 = \begin{pmatrix} \sin \Theta_0 \\ -\cos \Theta_0 \end{pmatrix}, \tag{10.7}$$

i.e. $\xi(x_{N+1}^-) = \ln ||\Pi_N||_{\Psi_0}$. We also introduce another possible definition of the norm

$$|||\Pi_N||| = \int_{|\Psi_0|=1} d\Psi_0 ||\Pi_N||_{\Psi_0}, \tag{10.8}$$

closer to the spirit of (10.6).

For $\varepsilon = 0$, the matrix product Π_N can be studied rather directly: the angles vanish $\theta_n = 0$ and the matrices M_n commute. Hence we can write

$$\Pi_N = \begin{pmatrix} e^\Lambda & 0 \\ 0 & e^{-\Lambda} \end{pmatrix} \text{ with } \Lambda = \sum_{n=1}^N \eta_n. \tag{10.9}$$

The distribution of the random variable Λ is given by the central limit theorem: $\langle \Lambda \rangle = \rho x \langle \eta_n \rangle = 0$ and $\text{Var}(\Lambda) = \rho x \langle \eta_n^2 \rangle = gx$ (we consider that x is fixed and N fluctuates with $\langle N \rangle = \rho x$). We have

$$\ln ||\Pi_N||_{\Psi_0} = \frac{1}{2} \ln [\cosh 2\Lambda - \cos 2\Theta_0 \sinh 2\Lambda]. \tag{10.10}$$

We examine first the particular case $\Theta_0 = 0$, leading to $\ln ||\Pi_N||_{\Psi_0} = -\Lambda$. We immediatly deduce that $\langle \ln ||\Pi_N||_{\Psi_0} \rangle = 0$ and $\text{Var}(\ln ||\Pi_N||_{\Psi_0}) = gx$, which would lead to $\gamma_1 = 0$ and, incorrectly, to $\gamma_2 = g$. The choice $\Theta_0 = \pi/2$ leads to a similar conclusion. This reflects the statistical properties of the two particular zero energy solutions

$$\begin{pmatrix} 1 \\ 0 \end{pmatrix} e^{\int^x dx' m(x')} \text{ and } \begin{pmatrix} 0 \\ 1 \end{pmatrix} e^{-\int^x dx' m(x')} \tag{10.11}$$

selected by the choices $\Theta_0 = \pi/2$ and $\Theta_0 = 0$, respectively.

We now consider the case of an arbitrary initial vector, with $\Theta_0 \notin \{0, \pi/2\}$. In the $N \rightarrow \infty$ limit, the large Λ behaviour of the norm is selected: $\ln ||\Pi_N||_{\Psi_0} \simeq |\Lambda| + \theta_H(\Lambda) \ln |\sin \Theta_0| + \theta_H(-\Lambda) \ln |\cos \Theta_0|$. Some algebra gives, for $gx \gg 1$,

$$\langle \ln ||\Pi_N||_{\Psi_0} \rangle \simeq \sqrt{\frac{2gx}{\pi}} + \frac{1}{2} \ln \left| \frac{1}{2} \sin 2\Theta_0 \right| \tag{10.12}$$

and

$$\text{Var}(\ln ||\Pi_N||_{\Psi_0}) \simeq gx \left(1 - \frac{2}{\pi} \right) + \frac{1}{4} \ln^2 |\tan \Theta_0|. \tag{10.13}$$

Note that the average value is reminiscent of the average of the logarithm of the transmission probability [27] (this calculation was first performed in Ref. [34] in another context). Interestingly, the behaviours (10.12, 10.13) were shown to persist in a quasi-1D situation with an odd number of channels (see the review [35] and references therein). We obtain

$$\gamma_1 = 0 \tag{10.14}$$

$$\gamma_2 = g \left(1 - \frac{2}{\pi} \right) = g \times 0.363380... \tag{10.15}$$

We can easily repeat this calculation with the second norm. Averaging of (10.10) over the angle Θ_0 gives

$$|||\Pi_N||| = \frac{2e^{|\Lambda|}}{\pi} \mathbf{E} \left(\sqrt{1 - e^{-4|\Lambda|}} \right), \tag{10.16}$$

where $\mathbf{E}(k)$ is the elliptic integral [36]. We deduce the asymptotic behaviours $\ln |||\Pi_N||| \simeq (3/4)\Lambda^2$ for $|\Lambda| \ll 1$ and $\ln |||\Pi_N||| \simeq |\Lambda| - \ln(\pi/2)$ for $|\Lambda| \gg 1$, leading again to (10.14, 10.15).

In conclusion: for $\varepsilon \neq 0$, the calculation of the cumulants γ_n is insensitive to the precise definition of the norm, i.e. to the precise choice of the initial spinor. In the Monte Carlo simulation, we have chosen $\Theta_0 = 0$ in order to set a Dirichlet boundary condition for the first component of the spinor. On the other hand, setting $\varepsilon = 0$, the behaviour of γ_2 as a function of Θ_0 presents two discontinuities precisely at 0 and $\pi/2$. We understand these singular values as resulting from a lack of ergodicity in the matrix space when considering the Abelian subgroup describing the case $\varepsilon = 0$. Hence, the value g found for $\Theta_0 = 0$ or $\pi/2$ should not be taken as the correct result.

Appendix 3: Two Other Subgroups of Random Matrices of $SL(2, \mathbb{R})$

It is well-known that the random Kronig–Penney model $[-\partial_x^2 + \sum_n v_n \delta(x - x_n)]\psi(x) = E \psi(x)$ for energy $E = k^2$ is controlled by transfer matrices of the form

$$M_n = \begin{pmatrix} \cos \theta_n & -\sin \theta_n \\ \sin \theta_n & \cos \theta_n \end{pmatrix} \begin{pmatrix} 1 & u_n \\ 0 & 1 \end{pmatrix} \tag{10.17}$$

where $\theta_n = k(x_{n+1} - x_n) > 0$ and $u_n = v_n/k$. The Schrödinger equation with negative energy $E = -k^2$ involves matrices of the form [16]

$$M_n = \begin{pmatrix} \cosh \theta_n & \sinh \theta_n \\ \sinh \theta_n & \cosh \theta_n \end{pmatrix} \begin{pmatrix} 1 & u_n \\ 0 & 1 \end{pmatrix} \tag{10.18}$$

with the same definitions for θ_n and u_n .

The study of the continuum limit, $\ell_n \rightarrow 0$ and $v_n \rightarrow 0$ with $\langle v_n \rangle = 0$ and $\sigma = \langle v_n^2 \rangle / \langle \ell_n \rangle$ fixed can be done along the same lines as in the paper. In this more simple case, the Riccati variable $z(x) = \psi'(x)/\psi(x)$ obeys the SDE $z'(x) = -E - z(x)^2 + V(x)$. In the continuum limit $V(x)$ is a Gaussian white noise of variance σ and the process is characterised by the (backward) generator $\mathcal{G} = (\sigma/2)\partial_z^2 - (E + z^2)\partial_z$. We arrive at

$$\gamma_2 = 2 \int dz dz' z G(z|z') z' f(z') \tag{10.19}$$

where

$$f(z) = \frac{2N}{\sigma} f_0(z) \int_{-\infty}^z \frac{dt}{f_0(t)} \text{ with } f_0(z) = e^{-\frac{2}{\sigma}\mathcal{U}(z)} \tag{10.20}$$

is the stationary distribution, involving the potential $\mathcal{U}(z) = Ez + (1/3)z^3$ and the integrated density of states $N(E)$, given in Ref. [37] for instance (also recalled in Ref. [25]). The equation

$$\mathcal{G}^\dagger G(z|z') = f(z) - \delta(z - z') \tag{10.21}$$

for the propagator can be solved:

$$G(z|z') = \frac{1}{N(E)} \left\{ f(z) \left[c(z') + \int_{-\infty}^z dt f(t) \right] - f_0(z) \int_{-\infty}^z dt \frac{f(t)^2}{f_0(t)} + \frac{f_0(z_>)f(z_<)}{f_0(z')} \right\} \tag{10.22}$$

where

$$c(z') + \frac{1}{2} = \frac{\sigma}{2N(E)} \left[\int_{-\infty}^{+\infty} dz'' f(z'')^2 f(-z'') - f(-z') f(z') \right] - \int_{-\infty}^{z'} dz'' f(z''). \tag{10.23}$$

We can analyse the limiting behaviours of the variance (10.19). In the high energy regime, $k = \sqrt{E} \gg \sigma^{1/3}$ we obtain the expansions

$$f(z) = \frac{k/\pi}{z^2 + k^2} + \frac{\sigma k}{\pi} \frac{z}{(z^2 + k^2)^3} + \mathcal{O}(\sigma^2) \tag{10.24}$$

(recall that $N(E) = k/\pi + \mathcal{O}(\sigma^2)$) and

$$G(z|z') = \left[\frac{1}{z^2 + k^2} + \sigma \frac{z}{(z^2 + k^2)^3} \right] \Omega(z, z') + \frac{3\sigma}{16\pi k^3} \left(\frac{1}{z^2 + k^2} - \frac{4k^4}{(z^2 + k^2)^3} \right) + \frac{\theta_H(z - z')}{z'^2 + k^2} \frac{f_0(z)}{f_0(z')} + \mathcal{O}(\sigma^2) \tag{10.25}$$

where

$$\Omega(z, z') = \frac{1}{2} \text{sign}(z' - z) + \frac{1}{\pi} \left[\arctan(z/k) - \arctan(z'/k) \right]. \tag{10.26}$$

When introducing these expressions in (10.19), the term $\mathcal{O}(\sigma^0)$ seems at first sight logarithmically divergent but is eliminated by symmetry (i.e. integrals must be understood as principal parts). We get

$$\gamma_2 = \frac{k\sigma}{\pi} \int dz \frac{z^2}{[U'(z)]^3} + \mathcal{O}(\sigma^2) = \frac{\sigma}{8E} + \mathcal{O}(\sigma^2) \tag{10.27}$$

i.e. we have recovered the asymptotic relation $\gamma_2 \simeq \gamma_1$ for $E \rightarrow \infty$ (SPS).

For $E = 0$, the fluctuations are finite $\gamma_2 = \tilde{c} \sigma^{1/3}$ where \tilde{c} is a dimensionless constant of order unity (calculated explicitly in Ref. [33]). γ_2 is maximum for a negative value of the energy, however the numerics shows that the ratio γ_2/γ_1 reaches its maximum at $E = 0$ (Fig. 5).

The limit $k = \sqrt{-E} \gg \sigma^{1/3}$ is more easy to handle. In this case the potential $U(z)$ develops a deep well at $z = k$, where the process is most of the “time” trapped. This dominates the fluctuations, which are those of the Ornstein–Uhlenbeck process,

$$\gamma_2 \underset{E \rightarrow -\infty}{\simeq} \frac{\sigma}{4(-E)}. \tag{10.28}$$

The fluctuations thus decay *faster* as energy decreases than in the Dirac case studied in the paper, since the relation between the two models involves the mapping $E \leftrightarrow \varepsilon^2$. Recalling that $\gamma_1 \simeq \sqrt{-E}$ in this case shows that $\gamma_2 \ll \gamma_1$ (no SPS).

Monte Carlo simulations are in perfect agreement with these behaviours (see Fig. 5).

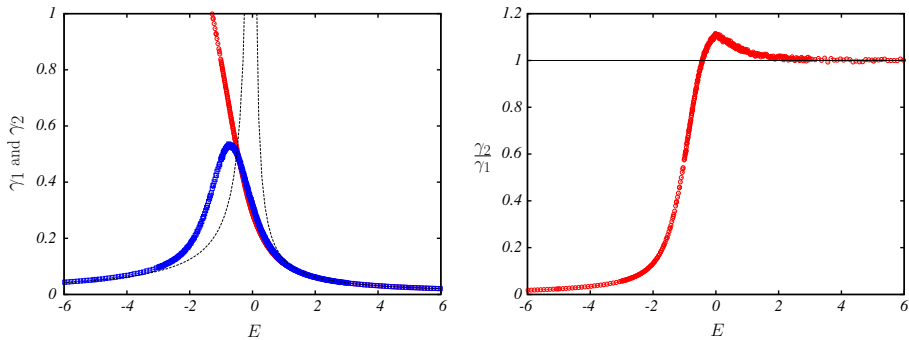


Fig. 5 (Color online) *Left* Plot of the Lyapunov exponent (red circles) and the variance (blue squares) for $\sigma = 1$ obtained by Monte Carlo simulations. Comparison with limiting behaviours (10.27) and (10.28) (dashed black lines). *Right* SPS, $\gamma_2/\gamma_1 \simeq 1$, holds for $E \gg \sigma^{2/3}$

The problem considered in this appendix was studied earlier in Refs. [33,38] in another context and with a different method: the generalised Lyapunov exponent (2.2) is obtained as the largest eigenvalue of the operator $\mathcal{G}^\dagger + qz$ [7]. The perturbative treatment [33] gives an integral representation

$$\gamma_2 = 2 \int dz (z - \gamma_1) \varphi_1(z) \tag{10.29}$$

where

$$\varphi_1(z) = N \left(\frac{2}{\sigma} \right)^2 f_0(z) \int_{-\infty}^z \frac{dz'}{f_0(z')} \int_{-\infty}^{z'} dz'' (\gamma_1 - z'') f_0(z'') \int_{-\infty}^{z''} \frac{dz'''}{f_0(z''')}. \tag{10.30}$$

Although it is not straightforward to prove the equivalence between (10.19) and (10.29), they seem to give similar results (see Fig. 1 of Ref. [33]).

References

1. Baxter, R.J.: Exactly Solved Models in Statistical Mechanics. Academic Press, London (1982)
2. Bougerol, P., Lacroix, J.: Products of Random Matrices with Applications to Schrödinger Operators. Birkhäuser, Basel (1985)
3. Luck, J.-M.: Systèmes désordonnés unidimensionnels. CEA, collection Aléa Saclay, Saclay (1992)
4. Crisanti, A., Paladin, G., Vulpiani, A.: Products of Random Matrices in Statistical Physics, Springer Series in Solid-State Sciences, vol. 104. Springer, Berlin (1993)
5. Figge, M.T., Mostovoy, M.V., Knoester, J.: Critical temperature and density of spin flips in the anisotropic random-field Ising model. Phys. Rev. B **58**, 2626–2634 (1998)
6. Paladin, G., Vulpiani, A.: Anomalous scaling and generalized Lyapunov exponents of the one-dimensional Anderson model. Phys. Rev. B **35**, 2015–2020 (1987)
7. Paladin, G., Vulpiani, A.: Anomalous scaling in multifractal objects. Phys. Rep. **156**(4), 147–225 (1987)
8. Altshuler, B.L., Prigodin, V.N.: Distribution of local density of states and NMR line shape in a one-dimensional disordered conductor. Sov. Phys. JETP **68**(1), 198–209 (1989)
9. Texier, C., Comtet, A.: Universality of the Wigner time delay distribution for one-dimensional random potentials. Phys. Rev. Lett. **82**(21), 4220–4223 (1999)
10. Anderson, P., Thouless, D.J., Abrahams, E., Fisher, D.S.: New method for a scaling theory of localization. Phys. Rev. B **22**(8), 3519–3526 (1980)
11. Cohen, A., Roth, Y., Shapiro, B.: Universal distributions and scaling in disordered systems. Phys. Rev. B **38**(17), 12125–12132 (1988)

12. Deych, L.I., Lisyansky, A.A., Altshuler, B.L.: Single parameter scaling in one-dimensional localization revisited. *Phys. Rev. Lett.* **84**(12), 2678 (2000)
13. Schomerus, H., Titov, M.: Band-center anomaly of the conductance distribution in one-dimensional Anderson localization. *Phys. Rev. B* **67**, 100201 (2003)
14. Titov, M., Schomerus, H.: Nonuniversality of Anderson localization in short-range correlated disorder. *Phys. Rev. Lett.* **95**, 126602 (2005)
15. Comtet, A., Luck, J.-M., Texier, C., Tourigny, Y.: The Lyapunov exponent of products of random 2×2 matrices close to the identity. *J. Stat. Phys.* **150**, 13–65 (2013)
16. Comtet, A., Texier, C., Tourigny, Y.: Products of random matrices and generalised quantum point scatterers. *J. Stat. Phys.* **140**(3), 427–466 (2010)
17. Le Doussal, P., Monthus, C., Fisher, D.S.: Random walkers in one-dimensional random environments: exact renormalization group analysis. *Phys. Rev. E* **59**(5), 4795 (1999)
18. Texier, C., Hagendorf, C.: Effect of boundaries on the spectrum of a one-dimensional random mass Dirac Hamiltonian. *J. Phys. A* **43**, 025002 (2010)
19. Comtet, A., Texier, C.: One-dimensional disordered supersymmetric quantum mechanics: a brief survey. In: Aratyn, H., Imbo, T.D., Keung, W.-Y., Sukhatme, U. (eds.) *Supersymmetry and Integrable Models*, Lecture Notes in Physics, vol. 502, pp. 313–328. Springer, Berlin (1998) (also available as cond-mat/9707313)
20. Bouchaud, J.-P., Comtet, A., Georges, A., Le Doussal, P.: Classical diffusion of a particle in a one-dimensional random force field. *Ann. Phys. (N.Y.)* **201**, 285–341 (1990)
21. Comtet, A., Texier, C., Tourigny, Y.: Lyapunov exponents, one-dimensional Anderson localisation and products of random matrices. *J. Phys. A* **46**, 254003 (2013)
22. Gardiner, C.W.: *Handbook of Stochastic Methods for Physics, Chemistry and the Natural Sciences*. Springer, Berlin (1989)
23. Texier, C.: Quelques aspects du transport quantique dans les systèmes désordonnés de basse dimension. PhD thesis, Université Paris 6. http://lptms.u-psud.fr/christophe_texier/ (1999)
24. Bienaimé, T., Texier, C.: Localization for one-dimensional random potentials with large fluctuations. *J. Phys. A* **41**, 475001 (2008)
25. Grabsch, A., Texier, C., Tourigny, Y.: One-dimensional disordered quantum mechanics and Sinai diffusion with random absorbers. *J. Stat. Phys.* **155**, 237–276 (2014)
26. Lifshits, I.M., Gredeskul, S.A., Pastur, L.A.: *Introduction to the Theory of Disordered Systems*. Wiley, New York (1988)
27. Steiner, M., Chen, Y., Fabrizio, M., Gogolin, A.O.: Statistical properties of localization-delocalization transition in one dimension. *Phys. Rev. B* **59**(23), 14848–14851 (1999)
28. Steiner, M., Fabrizio, M., Gogolin, A.O.: Random mass Dirac fermions in doped spin-Peierls and spin-ladder systems: one-particle properties and boundary effects. *Phys. Rev. B* **57**(14), 8290–8306 (1998)
29. Czycholl, G., Kramer, B., MacKinnon, A.: Conductivity and localization of electron states in one dimensional disordered systems: further numerical results. *Z. Phys. B* **43**, 5–11 (1981)
30. Kappus, M., Wegner, F.: Anomaly in the band centre of the one-dimensional Anderson model. *Z. Phys. B* **45**(1), 15–21 (1981)
31. Derrida, B., Gardner, E.J.: Lyapunov exponent of the one dimensional Anderson model: weak disorder expansions. *J. Physique* **45**, 1283–1295 (1984)
32. Gogolin, A.A.: Electron localization and hopping conductivity in one-dimensional disordered systems. *Phys. Rep.* **86**(1), 1–53 (1982)
33. Schomerus, H., Titov, M.: Statistics of finite-time Lyapunov exponents in a random time-dependent potential. *Phys. Rev. E* **66**, 066207 (2002)
34. Comtet, A., Monthus, C., Yor, M.: Exponential functionals of Brownian motion and disordered systems. *J. Appl. Probab.* **35**, 255 (1998)
35. Brouwer, P.W., Mudry, C., Furusaki, A.: Transport properties and density of states of quantum wires with off-diagonal disorder. *Physica E* **9**, 333–339 (2001)
36. Gradshteyn, I.S., Ryzhik, I.M.: *Table of Integrals, Series and Products*, 5th edn. Academic Press, Boston (1994)
37. Halperin, B.I.: Green's functions for a particle in a one-dimensional random potential. *Phys. Rev.* **139**(1A), A104–A117 (1965)
38. Zillmer, R., Pikovsky, A.: Multiscaling of noise-induced parametric instability. *Phys. Rev. E* **67**, 061117 (2003)